AGU PUBLICATIONS

Geophysical Research Letters

RESEARCH LETTER
10.1002/2014GL059952

Key Points:
- We reconstructed the 6 ka desert extent from vegetation and sedimentary facies
- At 6 ka, most of the Eastern Desert was stable but the Western Desert was mobile
- The desert in China was greatly reduced at 6 ka compared to the present day

Supporting Information:
- Readme
- Supplementary Text

Correspondence to:
H. Wu,
haibin-wu@mail.iggcas.ac.cn

Citation:
Li, Q., H. Wu, Z. Guo, Y. Yu, J. Ge, J. Wu, D. Zhao, and A. Sun (2014), Distribution and vegetation reconstruction of the deserts of northern China during the mid-Holocene, *Geophys. Res. Lett.*, *41*, 5184–5191, doi:10.1002/2014GL059952.

Received 19 MAR 2014
Accepted 7 JUL 2014
Accepted article online 10 JUL 2014
Published online 23 JUL 2014

Distribution and vegetation reconstruction of the deserts of northern China during the mid-Holocene

Qin Li[1,2], Haibin Wu[1], Zhengtang Guo[1], Yanyan Yu[1], Junyi Ge[3], Jianyu Wu[1], Deai Zhao[4], and Aizhi Sun[2]

[1]Key Laboratory of Cenozoic Geology and Environment, Institute of Geology and Geophysics, Chinese Academy of Sciences, Beijing, China, [2]University of Chinese Academy of Sciences, Beijing, China, [3]Key Laboratory of Vertebrate Evolution and Human Origins of the Chinese Academy of Sciences, Institute of Vertebrate Paleontology and Paleoanthropology, Chinese Academy of Sciences, Beijing, China, [4]Faculty of Earth Sciences, China University of Geosciences, Wuhan, China

Abstract Desertification is potentially a serious threat to society, and therefore, it is critical to understand how deserts may respond to future climate change. The mid-Holocene (6 ± 0.5 ^{14}C ka) was warmer than present, and the distribution of deserts at this time may have implications for understanding their response to future warming. Here we reconstruct the distribution of deserts in northern China during the mid-Holocene by combining data on vegetation type and the sedimentary facies of aeolian deposits. The results demonstrate that during the mid-Holocene, the deserts retreated northwestward to the location of the modern 300 mm isohyet. Most of the Eastern Desert was stabilized with steppe or forest-steppe vegetation, whereas the Western Desert exhibited no significant change and remained mobile, occupied by desert vegetation. The deserts in northern China were greatly reduced during the mid-Holocene because of the enhancement of the East Asian summer monsoon in a warmer climate than today.

1. Introduction

The most recent report by the Intergovernmental Panel on Climate Change states that a doubling of the present-day atmospheric CO_2 concentration may cause the mean global land surface air temperature to rise by about 1.1 to 2.6°C during the 21st century [*Intergovernmental Panel on Climate Change,* 2013] and which is expected to cause severe ecological and environmental problems, especially in arid and semiarid areas [*Manabe and Wetherald*, 1986; *Sato et al.*, 2007]. Desertification seriously affects the livelihood of millions of people in Asia and Africa, and therefore, it is important to understand how deserts may change under future warming scenarios [*Schlesinger et al.*, 1990; *Reynolds et al.*, 2007]. The mid-Holocene (6 ± 0.5 ^{14}C ka B.P.) period was a relatively warm interval when the Northern Hemisphere received more insolation in summer and less in winter compared to today [*Berger*, 1978], and the mid-Holocene experienced a temperature rise that is comparable to projected increases due to global warming [*Kellogg*, 1978; *Joussaume and Taylor*, 1995; *Braconnot et al.*, 2007]. Furthermore, geological records [e.g., *Shi et al.*, 1993; *Prentice et al.*, 1996; *Bigelow et al.*, 2003] and climate simulations [e.g., *Ganopolski et al.*, 1998; *Braconnot et al.*, 2007] suggest that the mid-Holocene exhibited distinct variations in climate and vegetation, which greatly influenced the evolution of the deserts. Thus, increasing our understanding of the environmental variability of deserts during the mid-Holocene may be helpful for predicting their possible response to future climate change.

The deserts in northern China extend from central Asia and include most of the dry lands located in the marginal zone of the East Asian summer monsoon (EASM), where the vegetation ecosystem and the desert distribution are highly sensitive to climate changes [*Lu et al.*, 2005; *Sun et al.*, 2006]. There are several reconstructions of the desert distribution in China during the mid-Holocene [i.e., *Dong et al.*, 1997; *Sun et al.*, 1998; *Jin et al.*, 2001; *Lu et al.*, 2013; *Yang et al.*, 2013], and they generally agree that the deserts underwent a sharp contraction during the mid-Holocene compared to the present day. However, because most of this work is confined to certain regions with limited availability of sedimentary records and accurate dates, the distribution of desert boundaries varies between different studies, and this needs to be more thoroughly investigated. In addition, little is known about the nature of vegetation change in the

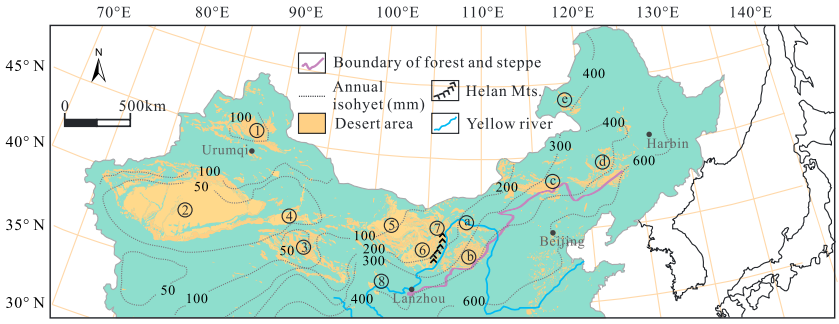

Figure 1. Location of desert landscapes, boundary between forest and steppe (information from *Zhang et al.* [2007]), and annual isohyets in northern China. (1: Gurbantunggut, 2: Taklamakan, 3: Kumtag, 4: Chaidamu, 5: Badain Jaran, 6: Tengger, 7: Wulanbuhe, 8: Gonghe, a: Kubuqi, b: Mu Us, c: Hunshandake, d: Horqin, and e: Hulunbeier.)

deserts of northern China, although this has a dramatic effect on sand mobility [*Lu et al.*, 2005; *Qiang et al.*, 2013] and desertification [*Sun*, 2000]. Although there are many vegetation reconstructions based on pollen analysis of individual sites in the dry lands of northern China [*Gao et al.,* 1992, 1993; *Jiang et al.*, 2006; *Yang et al.*, 2012; *Sun and Feng*, 2013], most of these studies focus on climate change over time rather than on spatial patterns.

In this study we used the quantitative method of biomization to reconstruct vegetation types during the mid-Holocene based on a synthesis of pollen data from all of the deserts and surrounding dry lands in northern China. Based on this reconstruction, we reconstructed the spatial distribution of deserts by combining the vegetation types with the sedimentary facies of aeolian deposits. The purpose of this study is to develop vegetation and desert distribution in northern China during the mid-Holocene and to provide insight for their possible future response to projected climate warming.

2. Data and Methods

2.1. Study Region

The deserts in northern China cover over 1.3×10^6 km^2 and are located between 35–50°N and 75–125°E [*Zhu et al.*, 1980]. In general, the deserts are located in the arid areas west of the Helan Mountains, known as the West Desert, whereas the sandy lands distributed in the semiarid regions east of the Helan Mountains are known as the East Sandy Land [*Zhu et al.*, 1980] (Figure 1).

The East Asian monsoon plays a significant role in controlling the hydrologic balance and effective moisture of the East Sandy Land [*Winkler and Wang*, 1993], while the West Desert is mainly controlled by the Northern Hemisphere westerlies [*Li*, 1990; *Vandenberghe et al.*, 2006]. Under the influence of the monsoon systems, the present-day annual rainfall decreases sharply from more than 400 mm in the eastern semiarid regions to below 50 mm in the northwestern arid regions (Figure 1), and the vegetation changes from temperate steppe to desert steppe and to desert.

2.2. Chronology

The BIOME 6000 project aims to reconstruct past vegetation patterns globally at 6000 ^{14}C yr B.P. (±500 year) and the Last Glacial Maximum, 18,000 ^{14}C yr B.P. (±1000 year), based on palaeoecological data and using a standard objective biomization technique [*Prentice et al.*, 1996; *Prentice and Webb*, 1998]. In this study, in order to correspond with BIOME 6000, the mid-Holocene was defined as 6 ± 0.5 ^{14}C ka B.P. The chronologies in the publications are based on optically stimulated luminescence (OSL), radiocarbon accelerator mass spectrometry (AMS ^{14}C), liquid scintillation radiocarbon (LSC ^{14}C), and thermoluminescence (TL) dating. Some of the dates (i.e., OSL and TL) are calendar dates and others (AMS ^{14}C and LSC ^{14}C) are uncalibrated ^{14}C dates. In order to obtain a consistent chronology, the radiocarbon dates were converted to calendar years using the CalPal2007 calibration curve [*Weninger et al.*, 2007], and thus, the mid-Holocene 6 ± 0.5 ^{14}C ka B.P. corresponds to 6.8 ± 0.5 calendar (cal) ka B.P.

The data used in this study are derived from lake sediments and aeolian deposits. Age-depth models for the pollen records from the lake sediments were estimated by linear interpolation between adjacent dates, while

the ages for mid-Holocene aeolian deposits were directly determined from the sample chronology or estimated using linear extrapolation between the nearest available dates in the same stratigraphic record. The quality of the dating control during the mid-Holocene was assessed by assigning a rank from 1 to 7, using ranking schemes from the Cooperative Holocene Mapping Project [*Webb*, 1985] (see the note in Table S1 in the supporting information). The dating controls for 88% of the pollen sites and 100% of the sedimentary facies records are better than 6D/3C (i.e., a single date with 2000 years or bracketing dates within 4000 years) (Table S1, Table S2, and Figure S1 in the supporting information).

2.3. Pollen and Sedimentary Sequences Data

A total of 35 pollen sites with 247 age controls (over 63% AMS ^{14}C, 35% LSC ^{14}C, and 1% OSL) (see Table S1 in the supporting information) covering the mid-Holocene period were obtained from the published literature from 1980 to 2013. We digitized the pollen diagrams and recalculated the percentages on the basis of the total number of terrestrial pollen types (excluding aquatic pollen and fern and algal spores). The pollen data were obtained on the basis of the constructed age models and consist of the nearest pollen spectrum to 6.0 ^{14}C ka (6.8 cal ka B.P.) within the permitted windows of 0.5 ka. This approach was preferred to interpolating between pollen spectra. If more than one sample fell within the designated window, multiple samples were averaged to produce the mid-Holocene pollen percentages.

A total of 81 sites with aeolian deposits with 459 age controls (75.8% OSL, 17.7% LSC ^{14}C, 4.8% AMS ^{14}C, and 1.7% TL) were selected from publications between 1980 and 2013 (see Table S2 in the supporting information). The definition of the mid-Holocene time slice for the sedimentary facies records followed the same protocol used for the pollen data.

2.4. Reconstruction of the Distribution of Mid-Holocene Vegetation and Desert

The vegetation in deserts strongly controls dune form and desertification by protecting the dunes from intensive deflation [*Yang et al.*, 2013] and soil loss [*Wolfe and Nickling*, 1993; *Castillo et al.*, 1997]. Episodes of weakened monsoonal circulation would have reduced moisture availability and consequently vegetation cover, resulting in the expansion of broad dune fields and desert [*Lu et al.*, 2005; *Qiang et al.*, 2013].

In this study, the vegetation was reconstructed by the biomization method using the classification of plant functional types and biomes in China [*Members of China Quaternary Pollen Data Base*, 2001] and was performed using 3P-base software [*Guiot and Goeury*, 1996].

The mid-Holocene desert distribution was reconstructed based on the vegetation and the sedimentary facies of aeolian deposits. The principles underlying our approach are as follows: First, the reconstructed vegetation is an effective tool for understanding the expansion and contraction of deserts. The desert becomes stabilized or contracts when the vegetation cover is enhanced and becomes mobile or expands when the vegetation cover deteriorates [*Lu et al.*, 2005]. For example, the change from desert to steppe vegetation, or from steppe to forest steppe, implies desert contraction, while a change to desert-type vegetation implies desert expansion. Second, the distribution of desert is indicated directly by the aeolian sedimentary sequences, including aeolian sand, paleosols, and/or loess. Aeolian sand represents dune-field dune buildup and/or desert expansion, whereas paleosols and/or loess indicate stabilization of dunes and desert contraction [*Qiu*, 1989; *Dong et al.*, 1994; *Qiang et al.*, 2013]. Finally, the spatial patterns of the mid-Holocene vegetation and desert distribution are presented using the ArcGIS software.

3. Results

The biome reconstruction (Figure 2a) illustrates the pattern of vegetation distribution during the mid-Holocene. The results demonstrate that the vegetation type in the deserts of northern China at this time was characterized by broadly longitudinal patterns from steppe (STEP) and forest (COMX = cool mixed forest or TEDE = temperate deciduous forest) in the east, to desert (DESE) in the northwest, similar to what is observed today. In the eastern part of the Helan Mountains, the vegetation was dominated by steppe; however, on the southern part of the East Sandy Land, there were a small number of sites with forest or forest-steppe vegetation. In detail, TEDE was scattered around the margin of Horqin, and numerous STEP sites are distributed in the northern areas, suggesting that the vegetation in Horqin was well developed. The Hulun

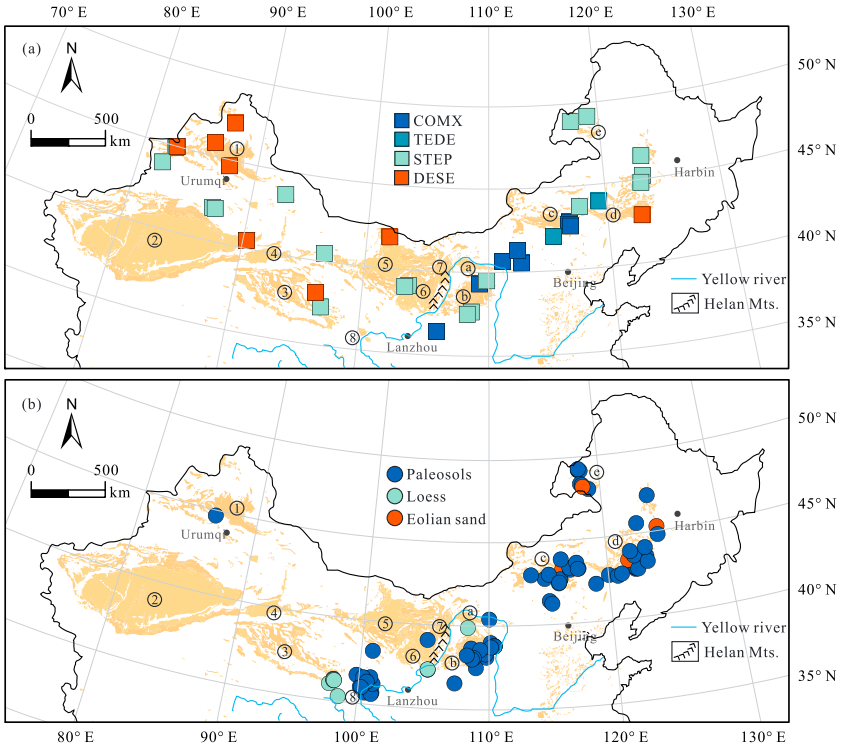

Figure 2. The characteristics of (a) vegetation and (b) sedimentary facies during the mid-Holocene period. Vegetation types: COMX: cool mixed forest, TEDE: temperate deciduous forest, DESE: desert, and STEP: steppe (1: Gurbantunggut, 2: Taklamakan, 3: Kumtag, 4: Chaidamu, 5: Badain Jaran, 6: Tengger, 7: Wulanbuhe, 8: Gonghe, a: Kubuqi, b: Mu Us, c: Hunshandake, d: Horqin, and e: Hulunbeier).

Buir was occupied by STEP. The pollen records from Hunshandake, which are mainly concentrated in the southeastern margin, are characterized by COMX and TEDE. It should be noted that the forest types (i.e., COMX or TEDE) present within the deserts actually consisted of wooded grassland or forest steppe, since steppe usually records the second highest biome score, close to the dominant forest type in the forest type sites. The pollen assemblages in the forest type sites are characterized by *Quercus*, *Betula*, *Pinus*, or *Ulmus*. The vegetation on the margin of the Kubuqi and Mu Us desert is characterized mainly by STEP.

In the western part of the Helan Mountains, all of the sites in Gurbantunggut are assigned the DESE type and several scattered DESE sites occurred solely at the margins of Taklamakan, Chaidamu, and Badain Jaran. Although there are two sites characterized by the STEP type west of Tengger, most of the STEP type usually occurs outside of these deserts. This may suggest that most of the West Desert was still dominated by DESE, which differs from the East Sandy Desert which was characterized by STEP or forest steppe during the mid-Holocene.

In Figure 2b, it can be seen that the records of sedimentary facies are distributed unevenly and are mainly located in East Sandy Land and Gonghe Sandy Land. In East Sandy Land, paleosols and loess are widely developed (93% of sites), which imply that the dunes were stabilized to a large extent as a result of vegetation development (Figure 2b). Aeolian sand (7% of sites) occurs only at scattered sites in Horqin, Hulun Buir, and Hunshandake, which may be attributed to the nature of specific local environments or to the unstable movement of aeolian sand [*Gao et al.*, 1993]. In the West Desert, records of aeolian deposits during the mid-Holocene are lacking. One paleosol site occurs at the northern edge of Tengger and another loess site in the southeastern part of Tengger (Figure 2b), which may imply that there was some degree of local environmental variability in the Tengger desert during the mid-Holocene. Although there is a paleosol site in Gurbantunggut, the vegetation in this area is still characterized by desert (Figure 2a), suggesting that it may still have been mobile in the mid-Holocene. There is still some degree of uncertainty regarding the extent of aeolian activity in the West Desert due to the limited number of sedimentological records for the mid-Holocene, and this area requires further investigation in the future. In addition, there was a widespread occurrence of paleosols and loess in the Gonghe Sandy Land.

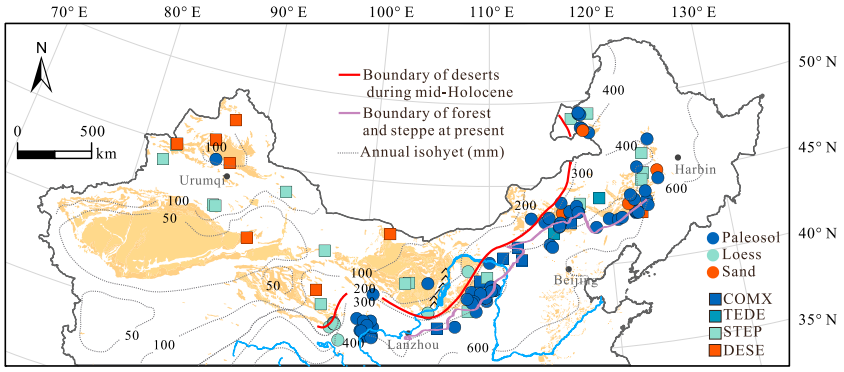

Figure 3. Coherent patterns of desert distribution during the mid-Holocene based on a combination of vegetation types and sedimentary facies. Vegetation types: COMX: cool mixed forest, TEDE: temperate deciduous forest, DESE: desert, and STEP: steppe.

4. Discussion

4.1. The Spatial Distribution of Deserts in Northern China During the Mid-Holocene

Combining the vegetation reconstructions with the sedimentary facies records produces a coherent picture of the spatial distribution of deserts in northern China during the mid-Holocene (Figure 3). The results indicate that the deserts generally retreated to close to the present-day 300 mm isohyet (Figure 3, the bold red line). Compared with the present-day distribution, most parts of the East Sandy Land, except for the western part of the Hunshandake and Mu Us deserts, exhibit a major westward retreat and were almost completely stabilized by STEP or forest steppe. In contrast, the West Desert exhibits no significant change and was still mobile; it was characterized by the DESE vegetation type. In particular, during the mid-Holocene, the boundary of the forest-steppe zone (a transitional vegetation from forest to steppe), the modern location of which corresponds to the 400 mm isohyet (the purple line in Figure 3), shifted westward to a location close to the present 300 mm isohyet (the bold red line in Figure 3).

We compared our reconstruction of the distribution of deserts during the mid-Holocene with the results of previous studies [*Dong et al.*, 1997; *Jin et al.*, 2001; *Zhou et al.*, 2002; *Lu et al.*, 2013] (Figure 4). There is a general agreement that the deserts exhibited a major northwestward contraction compared to their modern distribution. Nevertheless, there are some differences in detail: for example, for the mid-Holocene, *Zhou et al.* [2002] demonstrated that the southern desert margin shifted about 3° in latitude northward (to 41°N) (green dashed line in Figure 4); *Jin et al.* [2001] suggested that the desert/loess boundary moved about 250 km westward (pink dashed line in Figure 4); *Dong et al.* [1997] consider that the desert/loess boundary belt shifted northwestward to near the modern 200–300 mm annual isohyet (dark purple dotted line in Figure 4), and *Lu et al.* [2013] suggested that the East Sandy Land was almost completely stabilized and exhibited a major retreat while the margin of the West Desert exhibited a smaller change (blue dashed line in Figure 4).

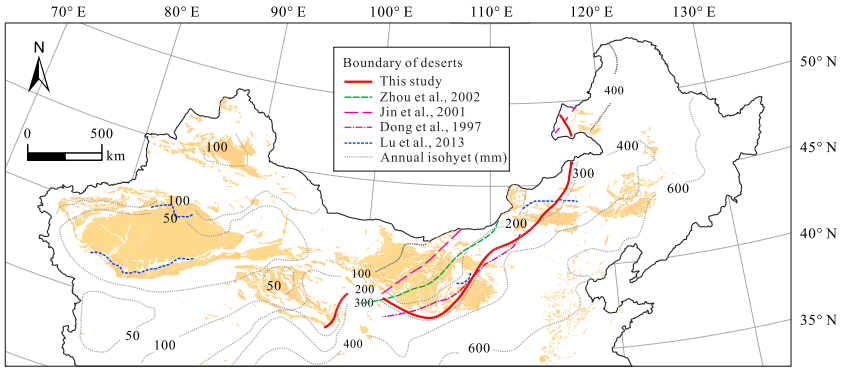

Figure 4. Comparison of the desert distribution during the mid-Holocene between this study and previous reconstructions.

However, our results suggest that the desert shifted northwestward to near the present-day 300 mm isohyet (bold red line in Figure 4), which suggests a degree of retreat which differs to that proposed by *Dong et al.* [1997], *Jin et al.* [2001], *Zhou et al.* [2002], and *Lu et al.* [2013].

The differences can be mainly attributed to the following reasons. First, there is a lack of consistency in previous studies in the definition of the mid-Holocene. For example, it was defined as 7.5–3 Ka B.P by *Jin et al.* [2001], 7.5–4 Ka B.P by *Dong et al.* [1997], and 9–5 Ka B.P by *Lu et al.* [2013]. This relatively broad range would have encompassed a significant amount of climatic variability resulting in corresponding differences in the location of the desert boundaries. In the present study, however, we used the strict definition of 6 ± 0.5 ^{14}C ka B.P. in order to allow for global comparisons. In addition, the distribution of the desert in northern China at 6 ± 0.5 ^{14}C ka B.P. provides an appropriate boundary condition for climate modeling. Second, a total of 81 sedimentary facies records with 459 age controls at 6 ± 0.5 ^{14}C ka B.P. were selected in this study from different publications, and these records represent relatively complete aeolian units covering the entire desert area in northern China. However, some of the previous studies [*Dong et al.*, 1997; *Jin et al.*, 2001; *Zhou et al.*, 2002] focused mainly on the desert-loess transition based on a limited number of sites: e.g., 10 sites in *Zhou et al.* [2002] and 9 sites in *Jin et al.* [2001]. Third, we suggest that our study represents a significant advance in that vegetation records that were combined with sedimentary facies records in order to reconstruct the spatial distribution of desert. In contrast, previous studies have focused mainly on sedimentary facies [*Dong et al.*, 1997; *Jin et al.*, 2001; *Zhou et al.*, 2002; *Lu et al.*, 2013]. Therefore, we suggest that our reconstruction provides a more comprehensive spatial distribution of desert in northern China during the mid-Holocene.

4.2. Mid-Holocene Moisture History in Northern China and Possible Forcing Mechanisms

The northwestward shift of the deserts in China in the mid-Holocene suggests that moisture levels were enhanced compared to the present day. In addition, a large amount of geological evidences based on various climate proxies, including magnetic susceptibility [*Peterse et al.*, 2011], pollen assemblages [*Jiang et al.*, 2006; *Wang and Feng*, 2013], total organic carbon content of lake sediments [*Xiao et al.*, 2006], and lake levels [*Yu et al.*, 2001], from the arid and semiarid regions of northern China suggests that the moisture level during the mid-Holocene was significantly greater than at the present day. In addition, the results of numerical climate models suggest that the mid-Holocene summer precipitation, and thus the EASM, was stronger in northern China than today [*Wang et al.*, 2010; *Zhou and Zhao*, 2010; *Jiang et al.*, 2013a, 2013b]. It has been proposed that an enhanced land-sea thermal contrast, and therefore an increased sea level pressure gradient between the East Asian continent and adjacent oceans, was responsible for the strengthening of the EASM during the mid-Holocene [*Jiang et al.*, 2013a]. The strengthened EASM resulted in increased moisture transport from the ocean to the inland deserts in northern China, in turn resulting in soil formation and vegetation development and thus to increased sand dune stability and desert contraction.

The global climate during the mid-Holocene is widely regarded to have been warmer than the present day [*Kaufman et al.*, 2004]. Although the Earth's orbital configuration, atmospheric greenhouse gas concentrations, and level of human activity were different to today, other boundary conditions such as ice sheet extent and sea level were similar [*Houghton et al.*, 1990; *Texier et al.*, 1997; *Bigelow et al.*, 2003]. Therefore, the mid-Holocene constitutes a potentially useful reference for a future warmer climate [*Bartlein et al.*, 2011]. Our results reveal that in northern China during the mid-Holocene, the deserts underwent a major northwestward retreat to a location near the present-day 300 mm isohyet. Understanding the dynamics of desert boundaries and their driving mechanisms at this time is crucial for assessing the possible response of these areas to projected future climate change.

Acknowledgments
This research was funded by the National Natural Science Foundation of China (41125011 and 41071055), the Bairen Programs of the Chinese Academy of Sciences, the Strategic Priority Research Program (XDA05120702), and the National Basic Research Program of China (973 Program, grant 2010CB950204). Data supporting Figure 2 are available in Table S1 and S2 in the supporting information.

The Editor thanks Slobodan Marković and an anonymous reviewer for their assistance in evaluating this paper.

References

Bartlein, P. J., et al. (2011), Pollen-based continental climate reconstructions at 6 and 21 ka: A global synthesis, *Clim. Dynam.*, *37*(3–4), 775–802, doi:10.1007/s00382-010-0904-1.

Berger, A. L. (1978), Long-term variations of daily insolation and quaternary climatic changes, *J. Atmos. Sci.*, *35*(12), 2362–2367, doi:10.1175/1520-0469(1978)035<2362:LTVODI>2.0.CO;2.

Bigelow, N. H., et al. (2003), Climate change and Arctic ecosystems: 1. Vegetation changes north of 55°N between the last glacial maximum, mid-Holocene, and present, *J. Geophys. Res.*, *108*(D19), 8170, doi:10.1029/2002JD002558.

Braconnot, P., et al. (2007), Results of PMIP2 coupled simulations of the Mid-Holocene and Last Glacial Maximum - Part 1: Experiments and large-scale features, *Clim. Past*, *3*(2), 261–277.

Castillo, V. M., M. MartinezMena, and J. Albaladejo (1997), Runoff and soil loss response to vegetation removal in a semiarid environment, *Soil Sci. Soc. Am. J.*, *61*(4), 1116–1121, doi:10.2136/sssaj1997.03615995006100040018x.

Dong, G. R., J. Jin, B. S. Li, S. Y. Gao, and Y. J. Shao (1994), Several problems on the desertification of Horqin Sandy Land, northeast china- A case study on its south area [in Chinese with English abstract], *J. Desert Res.*, *14*(1), 1–9.
Dong, G. R., H. L. Jin, and H. Z. Chen (1997), Desert-loess boundary belt shift and climatic change since the last interglacial period [in Chinese with English abstract], *Quaternary Sci.*, *2*, 158–167.
Ganopolski, A., C. Kubatzki, M. Claussen, V. Brovkin, and V. Petoukhov (1998), The influence of vegetation-atmosphere–ocean interaction on climate during the mid-Holocene, *Science*, *280*(5371), 1916–1919, doi:10.1126/science.280.5371.1916.
Gao, S. Y., H. L. Jin, W. N. Chen, and Y. F. Shi (1992), Mid-Holocene desert in China, in *Mid-Holocene Climates and Environments in China*, edited by Y. F. Shi and Z. C. Kong, pp. 161–167, China Ocean Press, Beijing, China.
Gao, S. Y., et al., (1993), A case study on desert evolution in the northwestern margin of monsoon area, China during the Holocene [in Chinese], *Sci. China Ser. B*, *23*(2), 202–208.
Guiot, J., and C. Goeury (1996), PPPBASE, a software for statistical analysis of paleoecological and paleoclimatological data, *Dendrochronologia*, *14*, 295–300.
Houghton, J. T., G. J. Jenkins, and J. J. Ephraums (1990), *Climate Change: The IPCC Scientific Assement*, Cambridge Univ. Press, Cambridge, U. K.
IPCC Working Group I-Twelfth session (2013), *The IPCC Fifth Assessment Report (AR5), Climate Change 2013: The Physical Science Basis*, IPCC, Stockholm, Sweden.
Jiang, W. Y., Z. T. Guo, X. J. Sun, H. B. Wu, G. Q. Chu, B. Y. Yuan, C. Hatte, and J. Guiot (2006), Reconstruction of climate and vegetation changes of Lake Bayanchagan (Inner Mongolia): Holocene variability of the East Asian monsoon, *Quaternary Res.*, *65*(3), 411–420, doi:10.1016/j.yqres.2005.10.007.
Jiang, D. B., X. M. Lang, Z. P. Tian, and L. X. Ju (2013a), Mid-Holocene East Asian summer monsoon strengthening: Insights from Paleoclimate Modeling Intercomparison Project (PMIP) simulations, *Palaeogeogr. Palaeocl.*, *369*, 422–429, doi:10.1016/j.palaeo.2012.11.007.
Jiang, D. B., Z. P. Tian, and X. M. Lang (2013b), Mid-Holocene net precipitation changes over China: model-data comparison, *Quaternary Sci. Rev.*, *82*, 104–120, doi:10.1016/j.quascirev.2013.10.017.
Jin, H. L., G. R. Dong, Z. Z. Su, and L. Y. Sun (2001), Reconstruction of the spatial patterns of desert/loess boundary belt in North China during the Holocene, *Chinese Sci. Bull.*, *46*(12), 969–974.
Joussaume S., Taylor K. E. (1995), Status of the Paleoclimate Moeling Intercomparison Project (PMIP), in Proceeding of the First International AMIP Scientific Conference (Monterey, California, U.S.A., 15–19 May 1995), WCRP Report, 92, pp. 425–430.
Kaufman, D. S., et al. (2004), Holocene thermal maximum in the western Arctic (0–180 W), *Quaternary Sci. Rev.*, *23*(5), 529–560, doi:10.1016/j.quascirev.2003.09.007.
Kellogg, W. W. (1978), Global influence of mankind on climate, in *Climate change*, edited by J. Gribben, pp. 205–227, Cambridge Univ. Press, Cambridge, U. K.
Li, J. J. (1990), The patterns of environmental changes since late pleistocene in northwestern China [in Chinese with English abstract], *Quaternary Sci.*, *3*, 197–204.
Lu, H. Y., X. D. Miao, Y. L. Zhou, J. Mason, J. Swinehart, J. F. Zhang, L. P. Zhou, and S. W. Yi (2005), Late Quaternary aeolian activity in the Mu Us and Otindag dune fields (north China) and lagged response to insolation forcing, *Geophys. Res. Lett.*, *32*, L21716, doi:10.1029/2005GL024560.
Lu, H. Y., et al. (2013), Chinese deserts and sand fields in Last Glacial Maximum and Holocene Optimum, *Chin. Sci. Bull.*, *58*(23), 2775–2783, doi:10.1007/s11434-013-5919-7.
Manabe, S., and R. T. Wetherald (1986), Reduction in summer soil wetness induced by an increase in atmospheric carbon-dioxide, *Science*, *232*(4750), 626–628, doi:10.1126/science.232.4750.626.
Members of China Quternary Pollen Data Base (2001), Simulation of China biome reconstruction based on pollen data from surface sediment samples [in Chinese with English abstract], *Acta Bot. Sin.*, *43*(2), 201–209.
Peterse, F., M. A. Prins, C. J. Beets, S. R. Troelstra, H. Zheng, Z. Gu, S. Schouten, and J. S. S. Damste (2011), Decoupled warming and monsoon precipitation in East Asia over the last deglaciation, *Earth Planet Sci. Lett.*, *301*(1–2), 256–264, doi:10.1016/j.epsl.2010.11.010.
Prentice, I. C., and T. Webb (1998), BIOME 6000: Reconstructing global mid-Holocene vegetation patterns from palaeoecological records, *J. Biogeogr.*, *25*(6), 997–1005, doi:10.1046/j.1365-2699.1998.00235.x.
Prentice, I. C., J. Guiot, B. Huntley, D. Jolly, and R. Cheddadi (1996), Reconstructing biomes from palaeoecological data: A general method and its application to European pollen data at 0 and 6 ka, *Clim. Dynam.*, *12*(3), 185–194, doi:10.1007/s003820050102.
Qiang, M. R., F. H. Chen, L. Song, X. X. Liu, M. Z. Li, and Q. Wang (2013), Late Quaternary aeolian activity in Gonghe Basin, northeastern Qinghai-Tibetan Plateau, China, *Quaternary Res.*, *79*(3), 403–412, doi:10.1016/j.yqres.2013.03.003.
Qiu, S. W. (1989), Study on the formation and evolution of horqin sandy land [in Chinese with English abstract], *Sci. Geogr. Sin.*, *9*(4), 317–328.
Reynolds, J. F., D. M. S. Smith, E. F. Lambin, B. Turner, M. Mortimore, S. P. Batterbury, T. E. Downing, H. Dowlatabadi, R. J. Fernández, and J. E. Herrick (2007), Global desertification: Building a science for dryland development, *Science*, *316*(5826), 847–851, doi:10.1126/science.1131634.
Sato, T., F. Kimura, and A. Kitoh (2007), Projection of global warming onto regional precipitation over Mongolia using a regional climate model, *J. Hydrol.*, *333*(1), 144–154, doi:10.1016/j.jhydrol.2006.07.023.
Schlesinger, W. H., J. Reynolds, G. L. Cunningham, L. Huenneke, W. Jarrell, R. Virginia, and W. Whitford (1990), Biological feedbacks in global desertification, *Science*, *247*(4946), 1043–1048, doi:10.1126/science.247.4946.1043.
Shi, Y. F., Z. C. Kong, S. M. Wang, L. Y. Tang, F. B. Wang, T. D. Yao, X. T. Zhao, P. Y. Zhang, and S. H. Shi (1993), Mid-Holocene climates and environments in China, *Global Planet. Change*, *7*(1), 219–233, doi:10.1016/0921-8181(93)90052-P.
Sun, A. Z., and Z. D. Feng (2013), Holocene climatic reconstructions from the fossil pollen record at Qigai Nuur in the southern Mongolian Plateau, *Holocene*, *23*(10), 1391–1402, doi:10.1177/0959683613489581.
Sun, J. M. (2000), Origin of eolian sand mobilization during the past 2300 years in the Mu Us Desert, China, *Quaternary Res.*, *53*(1), 78–88, doi:10.1006/qres.1999.2105.
Sun, J. M., Z. L. Ding, and T. S. Liu (1998), Desert distributions during the glacial maximum and climatic optimum: Example of China, *Episodes*, *21*(1), 28–31.
Sun, J. M., S. H. Li, P. Han, and Y. Y. Chen (2006), Holocene environmental changes in the central Inner Mongolia, based on single-aliquot-quartz optical dating and multi-proxy study of dune sands, *Palaeogeogr. Palaeocl.*, *233*(1–2), 51–62, doi:10.1016/j.palaeo.2005.09.016.
Texier, D., N. De Noblet, S. Harrison, A. Haxeltine, D. Jolly, S. Joussaume, F. Laarif, I. Prentice, and P. Tarasov (1997), Quantifying the role of biosphere-atmosphere feedbacks in climate change: Coupled model simulations for 6000 years BP and comparison with palaeodata for northern Eurasia and northern Africa, *Climate Dynam.*, *13*(12), 865–881.
Vandenberghe, J., H. Renssen, K. V. Huissteden, G. Nugteren, M. Konert, H. Y. Lu, A. Dodonov, and J. P. Buylaert (2006), Penetration of Atlantic westerly winds into Central and East Asia, *Quaternary Sci. Rev.*, *25*, 2380–2389, doi:10.1016/j.quascirev.2006.02.017.

Wang, W., and Z. D. Feng (2013), Holocene moisture evolution across the Mongolian Plateau and its surrounding areas: A synthesis of climatic records, *Earth Sci. Rev.*, *122*, 38–57, doi:10.1016/j.earscirev.2013.03.005.

Wang, T., H. J. Wang, and D. B. Jiang (2010), Mid-Holocene East Asian summer climate as simulated by the PMIP2 models, *Palaeogeogr. Palaeocl.*, *288*(1–4), 93–102, doi:10.1016/j.palaeo.2010.01.034.

Webb, T., III (1985), *A Global Paleoclimatic Data Base for 6000 yr B.P. DOE/EV/10097-6*, US Department of Energy, Washington, D. C.

Weninger, B., O. Jöris, and U. Danzeglocke (2007), Cologne Radiocarbon Calibration & Paleoclimate Research Package CalPal. [Available at http://www.calpal.de/.]

Winkler, M. G., and P. K. Wang (1993), The late Quaternary vegetation and climate of China, in *Global Climates Since the Last Glacial Maximum*, edited by H. Wright, pp. 221–261, Univ. of Minnesota Press, Minneapolis, Minn.

Wolfe, S. A., and W. G. Nickling (1993), The protective role of sparse vegetation in wind erosion, *Progr. Phys. Geogr.*, *17*(1), 50–68, doi:10.1177/030913339301700104.

Xiao, J. L., J. T. Wu, B. Si, W. D. Liang, T. Nakamura, B. L. Liu, and Y. Inouchi (2006), Holocene climate changes in the monsoon/arid transition reflected by carbon concentration in Daihai Lake of Inner Mongolia, *Holocene*, *16*(4), 551–560, doi:10.1191/0959683606hl950rp.

Yang, L. H., T. Wang, J. Zhou, Z. P. Lai, and H. Long (2012), OSL chronology and possible forcing mechanisms of dune evolution in the Horqin dunefield in northern China since the Last Glacial Maximum, *Quaternary Res.*, *78*(2), 185–196, doi:10.1016/j.yqres.2012.05.002.

Yang, X. P., X. L. Wang, Z. T. Liu, H. W. Li, X. Z. Ren, D. G. Zhang, Z. B. Ma, P. Rioual, X. D. Jin, and L. Scuderi (2013), Initiation and variation of the dune fields in semi-arid China - with a special reference to the Hunshandake Sandy Land, Inner Mongolia, *Quaternary Sci. Rev.*, *78*, 369–380, doi:10.1016/j.quascirev.2013.02.006.

Yu, G., S. P. Harrison, and B. Xue (2001), *Lake Status Records From China: Data Base Documentation*, pp. 240–241, China Meterological Press, Beijing, China.

Zhang, X. S., et al. (2007), *Vegetation Map of China and Its Geographic Pattern (Illustration of the Vegetation Map of the People's Republic of China (1:1000 000)*, Geology Press, Beijing, China.

Zhou, B. T., and P. Zhao (2010), Modeling variations of summer upper tropospheric temperature and associated climate over the Asian Pacific region during the mid-Holocene, *J. Geophys. Res.*, *115*, D20109, doi:10.1029/2010JD014029.

Zhou, W. J., J. Dodson, M. J. Head, B. S. Li, Y. J. Hou, X. F. Lu, D. J. Donahue, and A. J. T. Jull (2002), Environmental variability within the Chinese desert-loess transition zone over the last 20 000 years, *Holocene*, *12*(1), 107–112, doi:10.1191/0959683602hl525rr.

Zhu, Z. D., Z. Wu, S. Liu, and X. Di (1980), *An Outline of Chinese Deserts*, Science Press, Beijing, China.